Journal Pre-proof

On the Segregation Behavior and Influences of Minor Alloying Element Zr in Nickel-based Superalloys

Yang Zhou, Bo Wang, Shuping Li, Wentao Li, Kai Xu, Jiamiao Liang, Fei Zhou, Chentuo Wang, Jun Wang

PII: S0925-8388(21)04579-5

DOI: https://doi.org/10.1016/j.jallcom.2021.163169

Reference: JALCOM163169

To appear in: *Journal of Alloys and Compounds*
Revised date: 4 December 2021
Accepted date: 6

Please cite this article as: Yang Zhou, Bo Wang, Shuping Li, Wentao Li, Kai Xu, Jiamiao Liang, Fei Zhou, Chentuo Wang and Jun Wang, On the Segregation Behavior and Influences of Minor Alloying Element Zr in Nickel-based Superalloys, *Journal of Alloys and Compounds,* (2021) doi:https://doi.org/10.1016/j.jallcom.2021.163169

This is a PDF file of an article that has undergone enhancements after acceptance, such as the addition of a cover page and metadata, and formatting for readability, but it is not yet the definitive version of record. This version will undergo additional copyediting, typesetting and review before it is published in its final form, but we are providing this version to give early visibility of the article. Please note that, during the production process, errors may be discovered which could affect the content, and all legal disclaimers that apply to the journal pertain.

© 2021 Published by Elsevier.

On the Segregation Behavior and Influences of Minor Alloying Element Zr in Nickel-based Superalloys

Yang Zhou[*,1], Bo Wang[2], Shuping Li[2], Wentao Li[1], Kai Xu[1], Jiamiao Liang*[,1], Fei Zhou[1], Chentuo Wang[1], Jun Wang[*,1]

ORCID: Yang Zhou: 0000-0002-5543-9366

1. Shanghai Key Laboratory of Advanced High-temperature Materials and Precision Forming, Shanghai Jiao Tong University, No. 800, Dongchuan Road, Shanghai, 200240, China

2. Jiangsu Longda Superalloy Material Limited Company, Jiangsu, Wuxi, 214105, China

[*] Corresponding author: Yang Zhou, yzhou76@sjtu.edu.cn; Jiamiao Liang, jmliang@sjtu.edu.cn; Jun Wang, junwang@sjtu.edu.cn .

Abstract

In IN100 superalloys, Zr element was found to distribute along the interfacial boundaries between eutectic pools and the matrix in the form of $Ni_{11}Zr_9$ intermetallic compound, using time-of-flight secondary-ion-mass-spectrometry. Zr addition could effectively decrease the solidus temperature of IN100 alloys, affecting the solidification zone, which also promotes the formation of γ-γ' eutectics and influences the morphology of carbides.

Keywords: casting; superalloy; secondary ion mass spectroscopy (SIMS); minor alloying element; segregation.

Journal Pre-proof

1. Introduction

Nowadays, with the increasing demand for high-temperature heavy duty tasks, Ni-based superalloys have found their extensive applications in aggressive service conditions, such as aircraft-engine combustion chambers, power generation industries, where excellent high-temperature mechanical properties and hot-corrosion resistance is required[1,2]. The unique properties of Ni-based superalloys primarily attributed to the existence of an FCC Ni-based matrix (γ solid solution), strengthened by $L1_2$-Ni_3Al type (γ' phase) or $D0_{22}$-Ni_3Nb type (γ'' phase) precipitates, solute atoms as well as certain carbides[1,3]. During the manufacturing of Ni-based superalloys, alloying elements play essential roles in optimizing the microstructure and physical properties in order to satisfy the demanding performance requirements[1,4]. Comprehensive investigations have been performed to understand the influences of various alloying elements, including both major elements and minor (trace) elements, on the microstructure, precipitation behavior, structural properties in Ni-based superalloys[3,5–9].

Among these alloying constituents, minor elements are quite ubiquitous in polycrystalline superalloys. Although these elements correspond to quantities on the magnitude of several hundred ppm, their functions are quite significant and essential in determining the service performance, and can be either beneficial or harmful, depending on the compositions[2,10]. For instance, it has been widely reported that the existence of minor alloying elements-Zr and B, provides major improvements in

creep resistance and hot workability due to the stabilization of grain boundaries (GB) by Zr and B's segregation at GBs during solidification as well as the reduction of diffusion rates[10,11]. Besides, previous studies also state that the existence of Zr could act as a scavenger to reduce detrimental trace element, such as sulfur, exerting beneficial effects on the high-temperature properties[10,12,13].

Despite the long-standing studies of minor alloying element influences on the microstructure and mechanical properties, an in-depth investigation regarding the interaction mechanisms of Zr with major elements like Ni, Al etc. and phase components including γ and γ' phases in Ni-based superalloys is still lacking[14]. Among these problems, clarifying the distinct distribution of Zr within alloys becomes the major concern. Although it has been generally assumed that in Ni-based superalloys Zr tends to segregate to GBs or interfacial boundaries due to odd sizes and relatively low solubilities in γ/γ' phases, few direct experimental characterizations have been reported so far. Huang and Koo, S. Wang *et al.* used Auger electron spectrometry to determine the segregations of Zr in CM 247 LC and TM321 superalloys respectively, where Zr is found to segregate at interfaces between matrix and borides/carbides, and may dissolve into carbides or matrix[6,15]. J Zhang *et al.* found that in IN718C alloy Zr tends to segregate into Laves phases, using electron probe[16]. However, their work did not present clear morphology and accurate distributions of Zr-rich phases in superalloys.

Secondary Ion Mass Spectrometry (SIMS) is a useful technique in elemental detection and depth profiling for surface analysis. The high sensitivity would allow

for parts-per-million (ppm) detection, especially for light elements, such as B and H[17,18]. Time of Flight SIMS (TOF-SIMS) instrument was later developed. Other than quadrupole or magnetic sector analyzers on SIMS which could allow observation of only a few ions in one analysis, time of flight analyzers allow parallel acquisition of all ions within a given mass range. Using SIMS techniques, direct evidence of B distribution at GBs has already been reported by Walsh *et al.* back in 1975[19] and more recently, by Kontis *et al.* using Nano-SIMS, with a spatial resolution down to tens of nanometer[20]. Nevertheless, no detailed SIMS work has been expanded into the determination of Zr distributions by far.

In this work, the IN100 superalloy is used for investigation. This alloy was developed in the early 1960s, but is still widely used today as heat-resistant gas turbines parts in cast or powder metallurgy form[21]. The segregation of Zr element in IN100 is characterized using TOF-SIMS. The influences of Zr existence on the solidification character and microstructure are also studied.

2. Experimental procedures

The nominal composition of IN100 superalloy is shown in Table 1. The master alloy is smelted in a vacuum induction furnace, then re-melted and cast into 6 groups of tensile test bars with different Zr contents. The analysis content (mass fraction) of Zr element is controlled at 0, 500, 700, 900, 3000 and 5000 ppm, respectively.

Table 1. Nominal chemical composition of tested IN100 superalloy (in wt.%)

Element	Ni	Cr	Co	Mo	Al	Ti	Fe	V	B	Zr
Composition	Bal.	9.5	15.0	3.1	6.2	5.0	0.01	0.80	0.05	0~0.50

The effect of Zr on the solidification process was analyzed using a high-temperature comprehensive thermal analyzer (DSC) at a heating/cooling rate of 10℃/min. X-ray diffraction, optical microscope (OM), scanning electron microscope (SEM) are used to characterize the microstructure. A TESCAN GAIA3 SEM-FIB-TOF-SIMS instrument is employed for the detection of elemental distributions with a 30kV Ga+ primary ion beam. The mass spectrometry detection limit is 3 ppm and spatial resolution is 40 nm in horizontal direction and 3 nm in depth. The Zr-segregated area in IN100 samples is directly obtained using Focused Ion Beam, which is then observed in an FEI Talos F200X transmission electron microscope (TEM).

Journal Pre-proof

3. Results and discussions

Thermo-Calc® (TCNI 8 database) is used to simulate the solidification process and phase components of the IN100 alloys, as shown in supplementary Fig. S1 and S2. According to calculated results, the solidification and precipitation sequence of major phases in IN100 should be liquid → γ + γ' → carbides → σ. The experimental results from DSC measurements are summarized in supplementary Fig. S3. The evolution of

transition temperatures in IN100 alloys containing different Zr contents are presented in Fig. 1, which shows the comparisons between calculated predictions using Thermo-Calc and DSC measurements. It can be seen that both solidus and liquidus temperatures start to decrease after Zr additions, compared to samples without Zr. In DSC measurements, as shown in Fig. 1 b), for alloys containing Zr, with an increasing Zr content, the liquidus temperature varies from 1332.9℃ to 1330.4℃, which does not change much. Whereas an obvious decrease in the solidus temperature is observed from 1277.0℃ for Zr-500 down to 1263.5℃ for Zr-5000. The difference between liquidus and solidus temperature, ΔT, first decreases and then increases after reaching a minimum value of 54.9℃ at 700 ppm Zr. In calculated results, similar trends can be found according to Fig. 1 a), while the decrease in solidus temperature is more significant than experiments. The above results suggest that Zr addition can effectively decrease the solidus temperature while maintaining liquidus line at a certain value in IN100 alloys. Proper Zr content (~ 700 ppm) could narrow the solidification zone, which might indicate an improvement of casting fluidity.

Journal Pre-proof

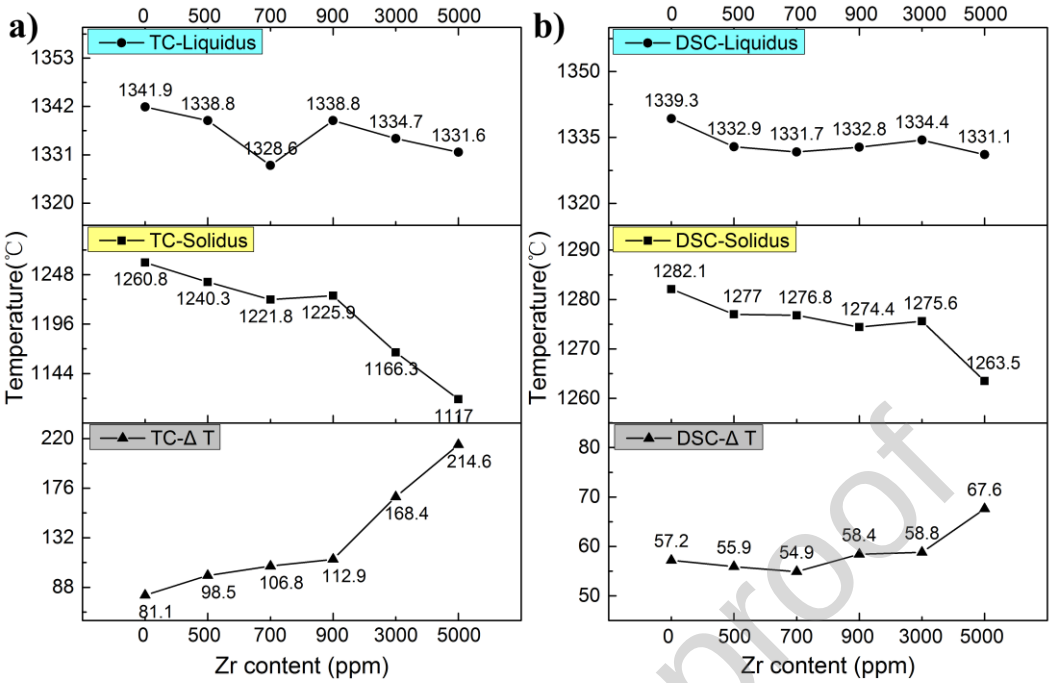

Figure 1. The evolution of transition temperatures in IN100 alloys containing different Zr contents: a) Thermo-Calc predictions; b) DSC measurements. $\Delta T=T_{liquidus}-T_{solidus}$.

Microstructural observations are conducted in order to analyze the grain size, precipitation/eutectic phase morphologies in IN100 alloys with different Zr contents. It can be seen from the metallographic images in Fig. 2 that IN100 alloys present typical as-cast columnar dendrite structure with interdendritic eutectics existing between the dendrites, mainly composing of γ and γ' phases. Besides, carbides with irregular morphologies, inclusions as well as porosity defects can be observed within the grains. In order to quantify the effects of Zr existence on the casting microstructure, the volume fractions of eutectic pools and micro-porosity are calculated based on the obtained metallographs of IN100 alloys with different Zr contents, as shown in Table 2. It shows that with increasing Zr content, the volume fractions of both eutectic pools and micro-porosity increases accordingly, where when

Zr content reaches over 3000 ppm, significant amount of eutectic regions (≥7.4%) and micropores (≥0.4%) can be observed.

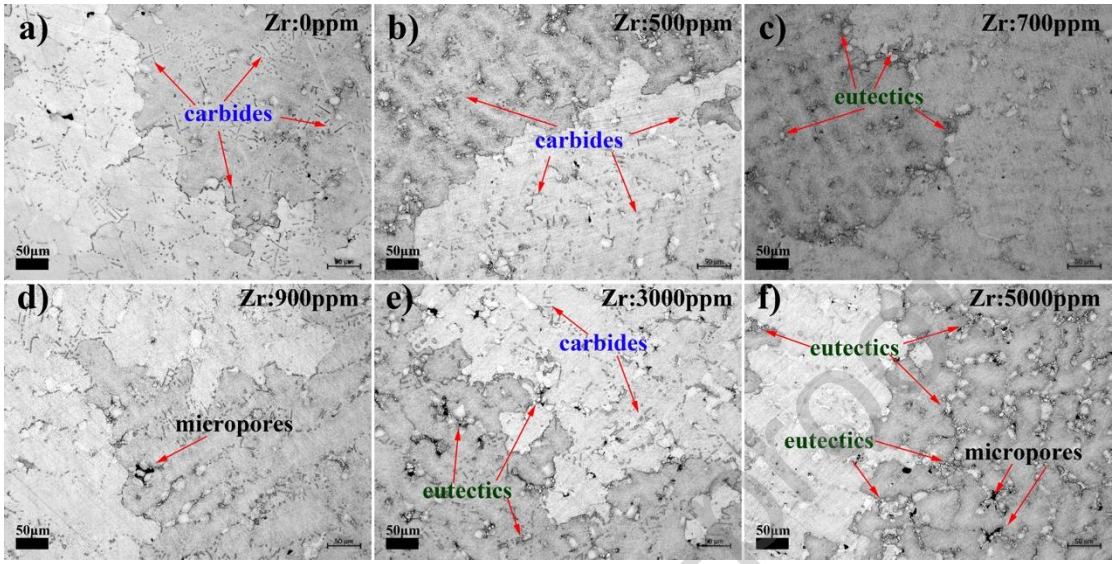

Figure 2. Optical microscope observations of IN100 alloys with different Zr contents: a) 0 ppm; b) 500 ppm; c) 700 ppm; d) 900 ppm; e) 3000 ppm; f) 5000 ppm.

Table 2. The volume fractions of eutectics and micropores in IN100 alloys with different Zr contents (in %)

Zr content(ppm) / Morphology	0	500	700	900	3000	5000
Eutectic pools	2.7%	3.4%	4.9%	5.2%	7.4%	12.9%
Micropores	0.1%	0.1%	0.2%	0.2%	0.4%	0.6%

SEM is used to further observe the morphology and structure of γ and γ' as well as other precipitated phases, as shown in Fig. 3. The most significant change is the

size of eutectic pools, which increases from 10~20 μm at low Zr content, to 60~80 μm when Zr content reaches over 3000 ppm. Combining metallographic observations, it can be concluded that the increasing Zr content leads to three main changes: 1) The volume fraction and size of interdendritic eutectics increases significantly; 2) Obvious shrinkage porosity defects start to appear at Zr = 900 ppm, and keep rising in quantity; 3) The carbide morphology also changes, varying from long script-like to particle-like pieces. Besides, in order to determine the specific crystal structure of phases in IN100 alloys, XRD analysis was performed and the result are presented in supplementary Fig. S2. The X-ray diffraction patterns show that all three samples (Zr content ranging from 500 to 900 ppm) show obvious γ and γ' diffraction peaks. Meanwhile, carbides (mainly, TiC phase) diffraction peaks are also indexed, indicating significant amount of carbides in IN100 alloys.

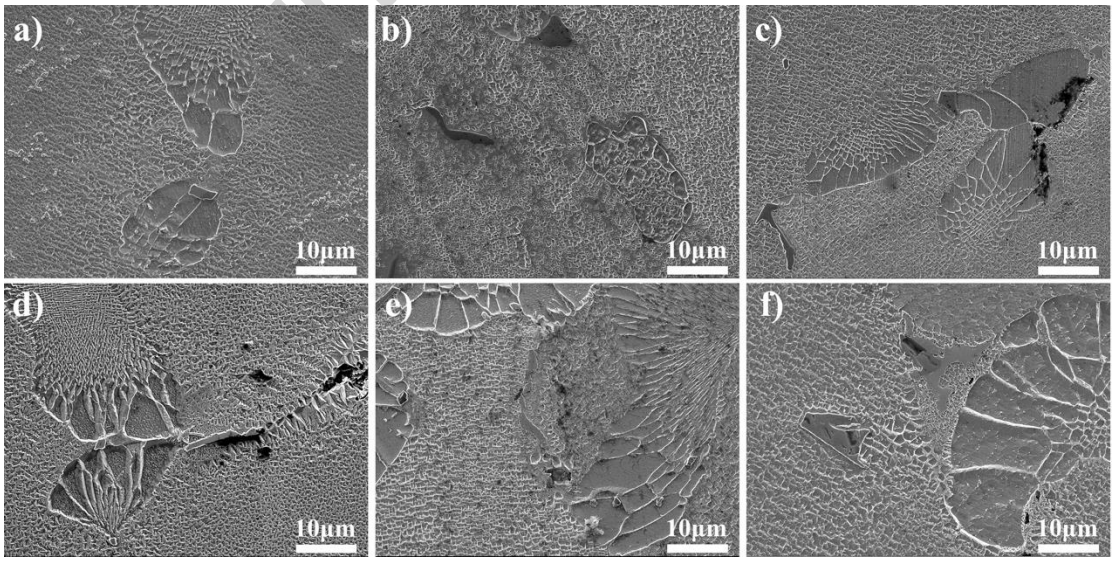

Figure 3. SEM observations of IN100 alloys with different Zr contents: a) 0 ppm; b) 500 ppm; c) 700 ppm; d) 900 ppm; e) 3000 ppm; f) 5000 ppm.

It is widely known that Zr element, although existing in trace amount, stills plays an important role in tuning the microstructure and mechanical properties in Ni-based superalloys. As has been mentioned above, previous reports regarding the determination of Zr segregations in superalloys fail to provide clear Zr-rich phase and accurate distributions, including EDS, AES, EPMA. Although atom-probe tomography has been reported to be useful in providing precise measurement of minor alloying elemental segregations, such as Zr and B, the detection area cannot be scaled up and thus overall distribution characterization is impossible[20,22]. As a result, in present work, TOF-SIMS analysis was employed and accurate distributing conditions of Zr element can been revealed accordingly, where typical regions are chosen and presented in Fig. 4. These representative elemental mappings indicate that the distribution of major composing elements can be clearly observed using TOF-SIMS at positive-ion mode, including Al, Ti, Ni, Cr and Mo. These major elements exhibit different segregation preferences in different phase areas, where Al and Ti tend to accumulate in the γ-γ' eutectic pools region while Ni and Cr prefer to stay in the γ matrix. The existence of Zr can also be distinctly observed, which tends to distribute along the edge of the sun-flowered eutectic pools area. Based on extensive observations and adequate analysis, we found that instead of the grain boundaries, Zr element prefers to stay with the interfacial boundaries between eutectics and the matrix, which include both intragranular and intergranular eutectics. This confirms the distinct segregations of minor alloying element Zr in IN100 Ni-based superalloys.

Meanwhile these findings do not contradict with previous assumptions that Zr tends to locate at GBs, e.g., as indicated in Fig. 4 c). But the segregation mechanism has been changed, not because of the existence of GBs, but due to the locations of eutectic pools at GBs.

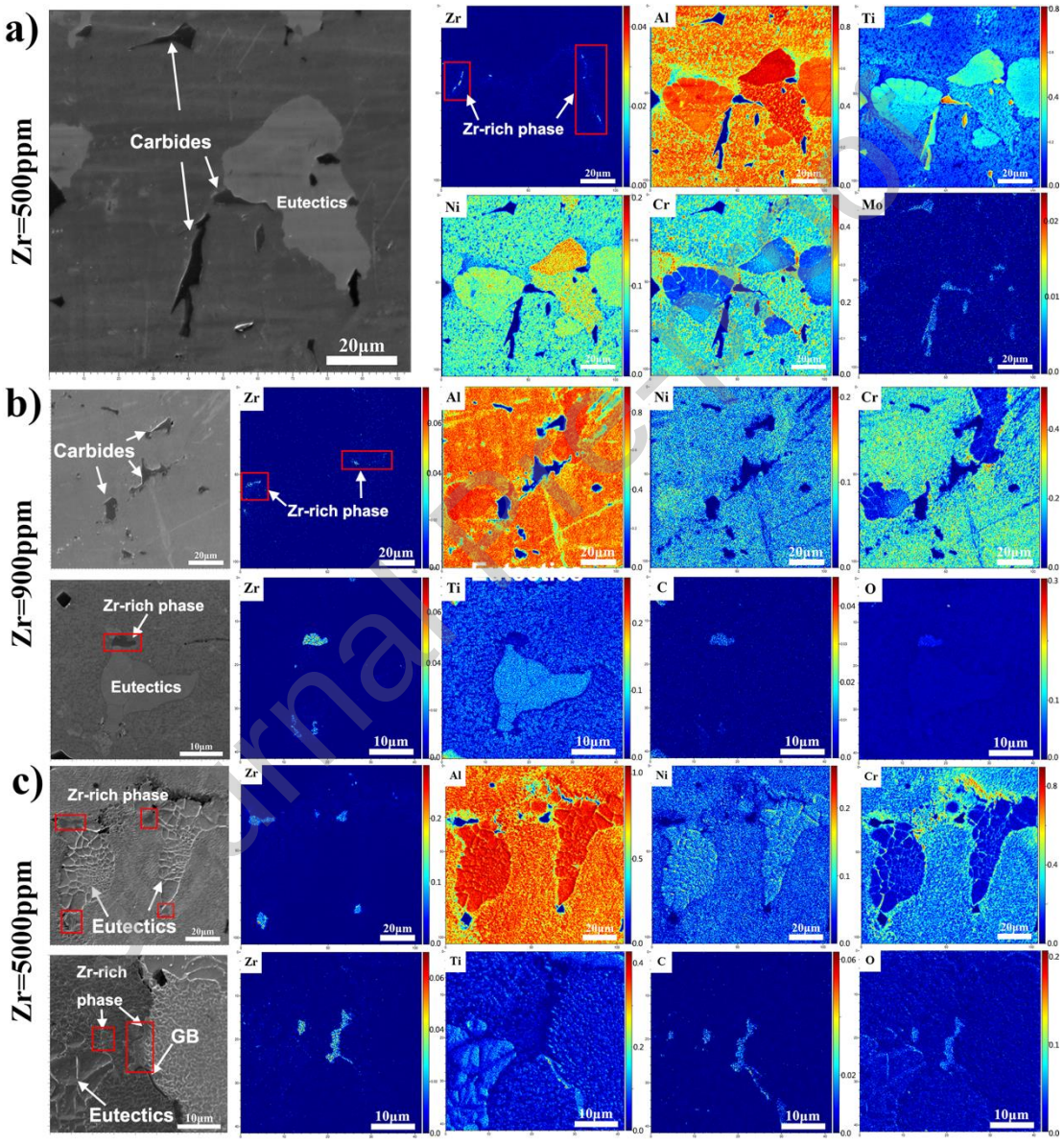

Figure 4. TOF-SIMS spectra indicating representative elemental distributions in IN100 alloys with different Zr contents: a) 500 ppm; b) 900 ppm; c)5000 ppm; b) and c) displayed elemental distributions at two magnifications: upper, 2000x and lower, 5000x.

In addition, Fig. 4 also implies that with increasing Zr content, the presence of Zr-rich phases becomes more significant, because the amount and average size of γ-γ' eutectic pools increase accordingly. In Fig. 4 b) and c), the magnified images (5K) of IN100 alloys with 900 ppm and 5000 ppm Zr show that in Zr-containing phases, C and O co-segregation is also observed, as determined under negative-ion mode in TOF-SIMS, suggesting that Zr could act as a gettering element for purifications of interfacial boundaries. Besides, elemental distributions of Chinese script Ti-carbides are also clearly displayed, where segregations of Ti and Mo elements are presented (Fig. 4 a)), indicating that apart from γ, γ' phases, significant amount of Ti carbides exist within IN100 alloys, in accordance with XRD analysis results.

Although elemental distributions can be distinctly obtained using TOF-SIMS technique, the exact composition of the target phase cannot be determined directly. Therefore, a specific Zr-containing area was obtained in-situ using FIB from IN100 alloy with 900 ppm Zr and analyzed subsequently with HR-TEM, as shown in Fig. 5 a). Fig. 5 b) shows the STEM image of IN100 alloy with Zr-containing region, where the morphology of Zr-rich phase can be clearly observed, exhibiting a thin curved-strip shape. In order to determine the crystal structure and atomic composition, selected area diffraction and EDS analysis were performed, as indicated in Fig. 5 b) and c) (point analysis results are listed in Table S1). Combining the SAED pattern (top-right one in Fig. 5 b)) and EDS point analysis results, a determination can be drawn, where the Zr-rich phase is identified as a $Ni_{11}Zr_9$ intermetallic compound

(Pearson Symbol: *tI40*), containing Ni and Zr, together with small amount of Al, Ti, Cr, C and O.

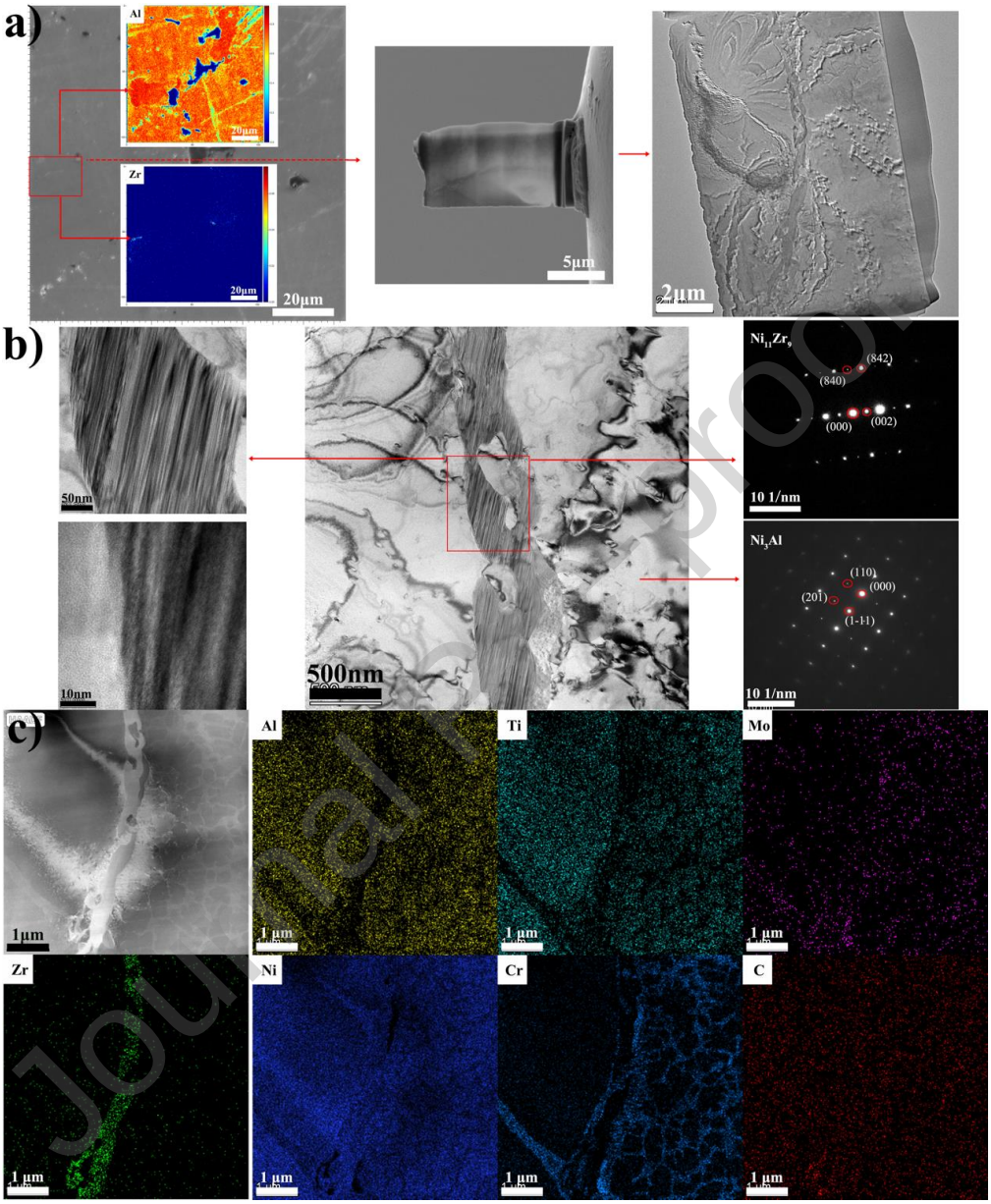

Figure 5. a) The selected site of interest for TEM observations in IN100 alloy containing 900 ppm Zr using FIB; b) TEM images of the FIB-machined sample and selected area electron diffraction patterns of the Zr-rich phase (upper) and the matrix (lower); c) Elemental distribution mappings of the Zr-rich phase with regard to Zr, Al, Ti, Mo, Ni, Cr and C, respectively.

From above experimental results, the influences of Zr content variation on the solidification behavior and as-cast microstructure can be clearly elucidated. According to Holt and Wallace, Zr element plays an effective role in depressing the solidus of Ni[10]. Therefore, an increase in Zr content would cause significant decrease in the solidus line of IN100 alloys, which affects solidification zones. Moreover, higher Zr would increase segregations in IN100 and promote γ-γ' eutectics formation, which has been theoreically explained by Zhou *et al.* in a Ni-Al system using effective distribution coefficient, k_e [23]. The result is also in good accordance with Wood's findings in IN738 castings[10]. Meanwhile, at high Zr content (> 900 ppm), the broadened mushy zone fails to provide sufficient feeding capacity, thus causing increased amount of micro-porosities and, possibly, deteriorated creep properties. Therefore, combining with DSC results analysis, an optimum Zr content of ~ 700 ppm is recommended and no higher than 900 ppm.

On the other hand, the preferred segregation behavior of Zr in IN100 alloys can also be explained. This relates to the fact that as surface active element, Zr could increase the volume fraction of residual liquid and thus promotes the fluidity[16], which can be verified from the decreased solidus temperature with increasing Zr content. Wherefore, when solidification occurs, due to a limited solubility in the matrix and eutectic pools, Zr gets segregated and precipitated, distributing around the last solidified, eutectic regions.

Journal Pre-proof

4. Conclusions

To sum up, in IN100 Ni-based superalloys, using TOF-SIMS analysis, we found that Zr element prefers to stay with the interfacial boundaries between eutectic pools and the matrix in the form of $Ni_{11}Zr_9$ intermetallic compound, which include both intragranular and intergranular eutectics. The addition of Zr could effectively decrease the solidus temperature of, affecting the solidification zone, which also promotes the formation of γ-γ' eutectics and influences the morphology of carbides.

This work confirms the distinct distribution and segregation behavior of Zr element in IN100 superalloys. The characterization method can be used to determine the presence and segregations of other essential minor/trace elements in superalloys, providing guidance for the metallurgical quality control in commercial superalloys.

Declaration of Competing Interest

The authors claim no conflict of interest.

Acknowledgement

This work is financially supported by the Project funded by National Science and Technology Major Project (2017-VI-0013-0085), National Natural Science Foundation of China (No. 52001205) and Shanghai Sailing Program (19YF1422600). The authors are grateful for the characterization work provided by Instrumental Analysis Center in Shanghai Jiao Tong University.

Data availability

The raw/processed data required to reproduce these findings cannot be shared at this time as the data also forms part of an ongoing study.

References

[1] A.K. Jena, M.C. Chaturvedi, The role of alloying elements in the design of nickel-base superalloys, J. Mater. Sci. 19 (1984) 3121–3139. https://doi.org/10.1007/BF00549796.

[2] G.W. Meetham, Trace elements in superalloys–an overview, Met. Technol. 11 (1984) 414–418. https://doi.org/10.1179/030716984803275188.

[3] F. Zhou, Y. Zhou, J. Wang, J. Liang, H. Gao, M. Kang, Enlightening from γ, γ′ and β phase transformations in Al-Co-Ni alloy system: A review, Curr. Opin. Solid State Mater. Sci. 23 (2019) 100784. https://doi.org/10.1016/j.cossms.2019.100784.

[4] M. Detrois, Z. Pei, K.A. Rozman, M.C. Gao, J.D. Poplawsky, P.D. Jablonski, J.A. Hawk, Partitioning of tramp elements Cu and Si in a Ni-based superalloy and their effect on creep properties, Materialia. 13 (2020) 100843. https://doi.org/10.1016/j.mtla.2020.100843.

[5] S. Floreen, J.M. Davidson, The effects of b and zr on the creep and fatigue crack growth behavior of a Ni-base superalloy, Metall. Trans. A. 14 (1983) 895–901. https://doi.org/10.1007/BF02644294.

[6] H.-E. Huang, C.-H. Koo, Effect of Zirconium on Microstructure and Mechanical Properties of Cast Fine-Grain CM 247 LC Superalloy, Mater. Trans. 45 (2004) 554–561. https://doi.org/10.2320/matertrans.45.554.

[7] S. Singh, R.K. Roy, B. Mahato, M. Ghosh, A. Mitra, A.K. Panda, Effect of Al incorporation for Co on the gamma-beta phase boundary of rapidly solidified CoNiAl ferromagnetic shape memory alloys, J. Magn. Magn. Mater. 368 (2014) 379–383.

Journal Pre-proof

[8] H.M. Medrano-Prieto, C.G. Garay-Reyes, M.A. Ruiz-Esparza-Rodriguez, I. Estrada, J.C. Guía-Tello, Q. Estrada, J.M. Silva-Aceves, J.S. Castro-Carmona, H. Camacho-Montes, R. Martínez-Sánchez, Influence of HIP Sintering and Ce/La Additions on the Microstructure and Hardness on Inconel 718 Nickel-based Superalloy, Microsc. Microanal. 26 (2020) 2914–2915. https://doi.org/10.1017/S1431927620023193.

[9] C. Wang, F. Zhou, Y. Zhou, M. Wang, J. Liang, J. Wang, B. Gan, Investigations of strength and ductility in Ni-xCo-10Al alloys via discontinuous precipitation, Mater. Charact. 163 (2020) 110318. https://doi.org/10.1016/j.matchar.2020.110318.

[10] R.T. Holt, W. Wallace, Impurities and trace elements in nickel-base superalloys, Int. Met. Rev. (1976) 1–24.

[11] D. Heydari, A.S. Fard, A. Bakhshi, J.M. Drezet, Hot tearing in polycrystalline Ni-based IN738LC superalloy: Influence of Zr content, J. Mater. Process. Technol. 214 (2014) 681–687. https://doi.org/10.1016/j.jmatprotec.2013.10.001.

[12] J. Zhang, R.F. Singer, Effect of Zr and B on castability of Ni-based superalloy IN792, Metall. Mater. Trans. A. 35 (2004) 1337–1342. https://doi.org/10.1007/s11661-004-0308-0.

[13] T.J. Garosshen, T.D. Tillman, G.P. McCarthy, Effects of B, C, and Zr on the structure and properties of a P/M nickel base superalloy, Metall. Trans. A. 18 (1987) 69–77. https://doi.org/10.1007/BF02646223.

[14] Z. Asqary, S.M. Abbasi, M. Seifollahi, M. Morakabati, The effect of boron and zirconium on the microstructure and tensile properties of Nimonic 105 superalloy,

Mater. Res. Express. 6 (2019) 116540. https://doi.org/10.1088/2053-1591/ab4676.

[15] Y.-L. Tsai, S.-F. Wang, H.-Y. Bor, Y.-F. Hsu, Effects of Zr addition on the microstructure and mechanical behavior of a fine-grained nickel-based superalloy at elevated temperatures, Mater. Sci. Eng. A. 607 (2014) 294–301. https://doi.org/10.1016/j.msea.2014.03.136.

[16] Z. Jie, J. Zhang, T. Huang, H. Su, Y. Zhang, L. Liu, H. Fu, Effects of boron and zirconium additions on the fluidity, microstructure and mechanical properties of IN718C superalloy, J. Mater. Res. 31 (2016) 3557–3566. https://doi.org/10.1557/jmr.2016.383.

[17] M. Kitajima, M. Fukutomi, M. Okada, Direct observation of boron diffusion using secondary ion mass spectrometry for SiC-coated molybdenum with a boron underlayer, Thin Solid Films. 105 (1983) 325–330. https://doi.org/10.1016/0040-6090(83)90315-2.

[18] K. Tsuruoka, K. Tsunoyama, Y. Ohashi, T. Suzuki, Application of the Ion Microprobe Mass Analyzer to Problems in Steels, Jpn. J. Appl. Phys. 13 (1974) 391. https://doi.org/10.7567/JJAPS.2S1.391.

[19] J.M. Walsh, B.H. Rear, Direct evidence for boron segregation to grain boundaries in a nickel-base alloy by secondary ion mass spectrometry, Metall. Trans. A. 6 (1975) 226–229. https://doi.org/10.1007/BF02673697.

[20] P. Kontis, H.A.M. Yusof, S. Pedrazzini, M. Danaie, K.L. Moore, P.A.J. Bagot, M.P. Moody, C.R.M. Grovenor, R.C. Reed, On the effect of boron on grain boundary character in a new polycrystalline superalloy, Acta Mater. 103 (2016) 688–699.

https://doi.org/10.1016/j.actamat.2015.10.006.

[21] A. Szczotok, Study of casting from IN100 nickel-based superalloy using quantitative metallography and analytical electron miroscopy: Untersuchung von Gussteilen aus hochlegierter IN100 Nickellegierung mittels quantitativer Metallographie und analytischer Elektronenmikroskopie, Mater. Werkst. 46 (2015) 320–329. https://doi.org/10.1002/mawe.201500408.

[22] A. Després, S. Antonov, C. Mayer, M. Veron, E.F. Rauch, C. Tassin, J.-J. Blandin, P. Kontis, G. Martin, Revealing the true partitioning character of zirconium in additively manufactured polycrystalline superalloys, Addit. Manuf. Lett. 1 (2021) 100011. https://doi.org/10.1016/j.addlet.2021.100011.

[23] P.J. Zhou, Y.U. Jin-Jiang, X.F. Sun, H.R. Guan, H.U. Zhuang-Qi, Roles of Zr and Y in cast microstructure of M951 nickel-based superalloy, Trans. Nonferrous Met. Soc. China. 22 (2012) 1594–1598.

Journal Pre-proof

Declaration of interests

☒ The authors declare that they have no known competing financial interests or personal relationships that could have appeared to influence the work reported in this paper.

☐The authors declare the following financial interests/personal relationships which may be considered as potential competing interests:

Journal Pre-proof